Dressed-State Resonant Coupling between Bright and Dark Spins in Diamond

C. Belthangady,[1,2] N. Bar-Gill,[1,2] L. M. Pham,[3] K. Arai,[4] D. Le Sage,[1,2] P. Cappellaro,[5] and R. L. Walsworth[1,2,*]

[1]*Harvard-Smithsonian Center for Astrophysics, 60 Garden Street, Cambridge, Massachusetts 02138, USA*
[2]*Department of Physics, Harvard University, Cambridge, Massachusetts 02138, USA*
[3]*School of Engineering and Applied Sciences, Harvard University, Cambridge, Massachusetts 02138, USA*
[4]*Department of Physics, Massachusetts Institute of Technology, Cambridge, Massachusetts 02139, USA*
[5]*Nuclear Science and Engineering Department, Massachusetts Institute of Technology, Cambridge, Massachusetts 02139, USA*

(Received 12 November 2012; published 12 April 2013)

Under ambient conditions, spin impurities in solid-state systems are found in thermally mixed states and are optically ''dark''; i.e., the spin states cannot be optically controlled. Nitrogen-vacancy (NV) centers in diamond are an exception in that the electronic spin states are ''bright''; i.e., they can be polarized by optical pumping, coherently manipulated with spin-resonance techniques, and read out optically, all at room temperature. Here we demonstrate a scheme to resonantly couple bright NV electronic spins to dark substitutional-nitrogen ($P1$) electronic spins by dressing their spin states with oscillating magnetic fields. This resonant coupling mechanism can be used to transfer spin polarization from NV spins to nearby dark spins and could be used to cool a mesoscopic bath of dark spins to near-zero temperature, thus providing a resource for quantum information and sensing, and aiding studies of quantum effects in many-body spin systems.

DOI: 10.1103/PhysRevLett.110.157601 PACS numbers: 76.30.Mi, 07.55.Ge, 72.25.−b

Nitrogen-vacancy (NV) color centers in diamond have attracted wide interest recently for applications in quantum information processing [1] and magnetometry [2–5]. Key characteristics of NV centers are their long electronic spin coherence lifetimes ($\sim$ ms) and their optically bright nature: i.e., the ability to prepare and read out NV spin states optically at room temperature. The diamond lattice is also host to many other dark spin impurities [6] i.e., electronic and nuclear spins that cannot be initialized or read out optically, and under ambient conditions are found in a thermal mixture of spin states. Fluctuating magnetic fields associated with this thermal bath of dark spins are a major source of decoherence for NV spins [7–12]. A key challenge is to couple and transfer polarization controllably from bright NV spins to dark spins both within and outside the diamond lattice, which can mitigate NV spin decoherence, convert the dark spins into a resource for quantum information [13,14] and sensing [15,16], and aid the study of quantum fluctuations and dynamics in many-body spin systems. Here, we use oscillating magnetic fields to dress and resonantly couple the electronic spin states of bright NV centers and dark substitutional-nitrogen ($P1$) defect centers. Such dressed-state resonant coupling can be used to realize optically controlled polarization transfer from bright NV spins to nearby dark spins, and thus effectively to cool a wide range of dark spin ensembles at room (and arbitrary) temperature.

Polarization of a solid-state dark-spin bath is possible at cryogenic temperatures and magnetic fields of several tesla [17], but has not been realized at room temperature. In previous experiments, coupling and electronic-spin polarization transfer between a single NV and a single proximal $P1$ center was demonstrated by tuning the static magnetic field B_0 to a level anticrossing [18,19]. However, when a diverse set of dark spins with different gyromagnetic ratios and/or hyperfine couplings is present, as is the case in typical diamond samples, such tuned-B_0 polarization transfer fails. Using dressed states for spin polarization transfer is robust in that it works at room temperature for any number of dark spin species, with magnetic fields that are both low ($\sim$mT) and user specified, and provides fast optical control. The $P1$ center, with its strong and orientation-dependent hyperfine coupling, exhibits a set of five optically dark electron spin resonance (ESR) transitions, and thereby serves as an ideal platform to demonstrate dressed-state resonant coupling to bright NV spins. As described below, we measured the spectral width of the NV-$P1$ resonant coupling interaction and the rate of polarization transfer between bright and dark spins, and thus established the conditions for optically controlled polarization (i.e., effective cooling) of mesoscopic dark spin ensembles in room-temperature diamond.

The essence of dressed-state resonant coupling is illustrated in Fig. 1(a). Two types of spins, A and B, with different gyromagnetic ratios (γ_A, γ_B) have unequal Zeeman splittings when placed in an external magnetic field (B_0) and therefore cannot exchange energy in the lab frame. However, if both sets of spins are driven resonantly at their respective Larmor frequencies with transverse oscillating magnetic fields (B_{1A} and B_{1B}) such that their Rabi frequencies are equal (analogous to the Hartmann-Hahn matching condition [20]), then in a double-rotating frame the dressed states of the two spins have equal energy separation and energy transfer becomes possible. If one of

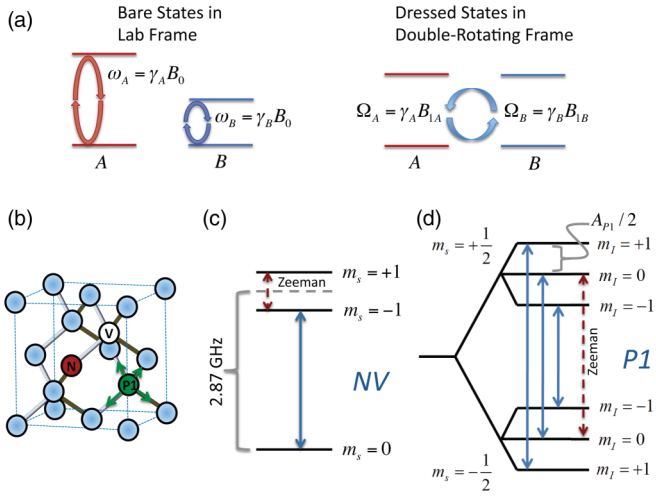

FIG. 1 (color online). Schematic of dressed-state resonant coupling and energy-level diagrams. (a) Two spins with dissimilar Zeeman splittings cannot exchange energy in the lab frame. When driven resonantly (red and blue circular arrows), energy exchange becomes possible. Dressed states in the double-rotating frame are separated by the spin Rabi frequencies controlled by the respective driving fields $B_{1A,B}$. When the Rabi frequencies are matched, i.e., $\Omega_A = \Omega_B$, energy conserving spin flip-flops can occur. (b) Nitrogen-vacancy (NV) and substitutional-nitrogen ($P1$) defects in diamond. Green arrows show the four possible orientations of the $P1$ hyperfine axis. (c) Ground electronic spin states of the negatively charged NV center. Degeneracy of the $|m_s = \pm 1\rangle$ states is lifted by application of a static magnetic field B_0 aligned parallel to the NV axis. Blue arrow denotes spin transition driven in the experiment. (d) Ground electronic spin states of the $P1$ defect. For B_0 oriented along the $\langle 111\rangle$ crystal direction, the hyperfine splitting is $A_{P1} = 114$ MHz when the hyperfine axis is parallel to B_0, and $A_{P1} = 90$ MHz for the three other orientations. Blue arrows indicate transitions driven in the experiment.

the species is spin polarized, this polarization may be transferred to the other species by means of a resonant flip-flop process in the double-rotating frame mediated by their mutual magnetic coupling. Dressed-state coupling has been studied for nuclear spins in bulk as well as nanoscale ensembles [21]. Modified dressed-state schemes have also been used to transfer thermal polarization from electronic to nuclear spins in bulk ensembles [22]. Here, we apply this technique to dissimilar electronic spins and demonstrate coupling between optically polarized spins of lower abundance (NV centers) and dark ($P1$) spins of higher abundance.

The NV center [see Fig. 1(b)] consists of a substitutional nitrogen atom and an adjacent vacancy in the diamond lattice. The ground state of the negatively charged NV center (the focus of the present work), shown in Fig. 1(c), is an electronic spin triplet ($S = 1$) with a zero-field splitting of 2.87 GHz. The degeneracy of the $|m_s = \pm 1\rangle$ states may be lifted with an external B_0 field and spin transitions between the Zeeman states can be driven by means of microwave radiation. Optical excitation at wavelengths shorter than the zero-phonon line at 638 nm leads to polarization of the NV electronic spin into the $|m_s = 0\rangle$ state. The $P1$ center consists of a nitrogen atom that has replaced one of the carbon atoms in the lattice [see Fig. 1(b)]. A Jahn-Teller distortion of one of the N-C bonds leads to an anisotropy in the hyperfine interaction between the $P1$ electronic spin and its nuclear spin (predominantly ^{14}N with $I = 1$). Figure 1(d) gives the energy level diagram of the $P1$ center and the three allowed electronic spin transitions. The hyperfine energy splitting is determined by the angle between the anisotropic hyperfine axis (the distorted N-C bond direction) and the static magnetic field, so that when B_0 is parallel to the $\langle 111\rangle$ crystal direction, the ESR spectrum of the $P1$ center comprises a set of five lines [17,23].

If the dark, thermally mixed $P1$ spins are brought into resonance with spin-polarized NVs, then polarization can be transferred from NVs to $P1$s mediated by the magnetic dipolar coupling with the Hamiltonian

$$H_{\rm dip} = \mathcal{D}_{{\rm NV},P1}\left[S_z^{\rm NV} S_z^{P1} - \frac{1}{4\sqrt{2}}(S_+^{\rm NV} S_-^{P1} + S_-^{\rm NV} S_+^{P1})\right]. \quad (1)$$

Here $\mathbf{S}^{\rm NV}$ and $\mathbf{S}^{P1}$ are the spin operators for the NV and $P1$ spins, respectively, $\mathcal{D}_{{\rm NV},P1} = \mu_0 \gamma_{\rm NV} \gamma_{P1} \hbar^2 (1 - 3\cos^2\theta)/4\pi r^3$ where r and θ are coordinates of the position vector connecting the spins, and $\gamma_{\rm NV} \approx \gamma_{P1} = 2\pi \times 2.8$ MHz/gauss. One method to bring the $P1$ and NV spins into resonance is to tune the static magnetic field to $B_0 = 512$ gauss. At this value of the field, the energy difference between the $|m_s = 0\rangle$ and $|m_s = -1\rangle$ NV spin states is equal to that between the $|m_s = -1/2, m_I = 0\rangle$ and $|m_s = 1/2, m_I = 0\rangle$ $P1$ spin states, and thus the second term of $H_{\rm dip}$ induces a resonant flip-flop process. However, this tuned B_0 technique fails when several $P1$ spins are strongly coupled to each NV (there are $\sim$10 to 1000 $P1$s per NV in typical diamond samples), because at a given B_0 field only one of the five $P1$ hyperfine transitions is on resonance with the NV. For the more generally applicable dressed-state scheme introduced here, the NV and $P1$ spins are locked in a direction transverse to the static B_0 field by controllable, continuous driving at microwave and rf frequencies, respectively. When the drive Rabi frequencies are matched, the NV and $P1$ spins are brought into resonance in a double-rotating frame, such that the dipolar Hamiltonian consists of only the first term of Eq. (1) [24]. This term $\sim S_z^{\rm NV} S_z^{P1}$ is perpendicular to the spin-locking direction and can therefore induce flip-flops between the $P1$ and NV spins. The primary advantage of dressed-state resonant coupling is that by driving each $P1$ hyperfine transition on resonance with a multifrequency rf field all five $P1$ transitions can be simultaneously brought into resonance with the NV in the rotating frame, allowing coupling and polarization transfer from the NV to all $P1$ spins. By direct analogy, bright NV spins can be coupled to

other dark (nuclear or electronic) spins with different Zeeman energies by driving each spin transition on resonance, simultaneously, and with matched Rabi frequencies. Other advantages of dressed-state resonant coupling include (i) the ability to switch on and off the coupling and polarization transfer mechanism on nanosecond time scales (by rapid switching of the rf and/or microwave fields), and (ii) the ability to couple bright and dark spins at any value of B_0.

Our experiments were performed using a home-built confocal microscope to interrogate a small ensemble ($\sim 10^4$) of NVs in a NV-dense diamond sample (see the Supplemental Material [25]). Applying Ramsey and Hahn-echo pulse sequences [24] to the NV $|m_s = 0\rangle \leftrightarrow |m_s = -1\rangle$ transition, we determined $T_2^* = 110(10)$ ns and $T_2 = 1.6(1)$ μs. To identify the resonance frequencies of the $P1$ spin bath we used the double-electron-electron-resonance sequence shown in Fig. 2(a) [11]. The frequency of the applied rf signal was swept to record the $P1$-bath ESR spectrum via the effect on the NV spin-echo fluorescence signal, as shown in Fig. 2(b). In addition to the $P1$ spectrum we found a double-electron-electron-resonance signal from an unknown electronic spin impurity (which is ubiquitous in all diamond samples we measured). We next set the frequency of the rf pulse to that of the central fluorescence dip, varied the width of the pulse, and recorded the NV spin-echo signal as an indicator of $P1$-bath Rabi oscillations [see Fig. 2(c)]. We then used a rf source outputting five frequencies to drive each of the five $P1$ ESR transitions, and adjusted the power at each frequency such that the Rabi frequency of every transition was equal to 8 MHz. We were thus able to drive collective, synchronized Rabi oscillations of the entire $P1$ spin bath.

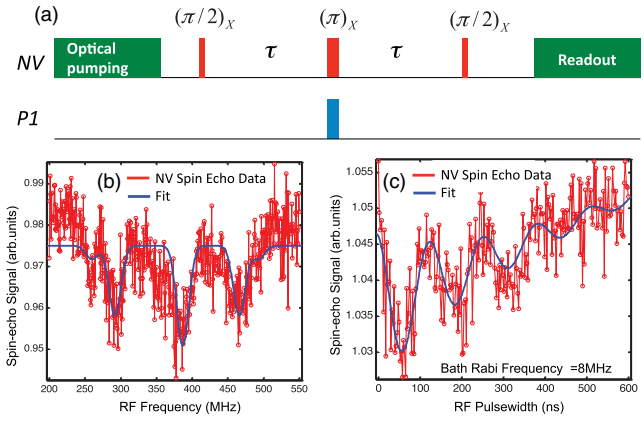

FIG. 2 (color online). Measured $P1$-bath ESR spectrum and Rabi oscillations. (a) NV optical and microwave (red) spin-echo sequence with a fixed free precession time of 350 ns is used to measure the $P1$ ESR spectrum and Rabi oscillations, for $B_0 = 128$ gauss. Coincident with the NV π pulse a 65-ns-long rf pulse (blue) is applied to the $P1$ bath spins. (b) $P1$-bath ESR spectrum is given by measured NV spin-echo fluorescence signal and NV-$P1$ dipolar coupling as the width of the $P1$ rf pulse is kept fixed and its frequency is swept. The $|m_s = -1/2, m_I = 0\rangle \leftrightarrow |m_s = 1/2, m_I = 0\rangle$ transition for all four $P1$ orientations yields the observed central NV fluorescence dip. The satellite dips are from the $|m_s = -1/2, m_I = \pm 1\rangle \leftrightarrow |m_s = 1/2, m_I = \pm 1\rangle$ transitions of off- and on-axis $P1$s. The small dip appearing on the shoulder of the central dip arises from other dark spins in the lattice [6,31]. Solid line represents a fit to a set of five Gaussians (see the Supplemental Material [25]). (c) With the frequency of the rf signal set to the central $P1$ resonance dip, the width of the rf pulse is swept to yield $P1$-bath Rabi oscillations via the effect of NV-$P1$ dipolar coupling on NV spin-echo fluorescence measurements. When the rf pulse width is 62.5 ns, the spin-echo signal is reduced due to an effective reversal of the dipolar field of the $P1$ bath. The rapid decay of oscillations is due to decoherence caused by dipolar coupling between $P1$ spins and ensemble averaging. Solid line is a fit to a decaying sinusoid (see the Supplemental Material [25]).

The pulse sequence we employed for dressed-state resonant coupling is shown in Fig. 3(a). The microwave power was adjusted to give a NV Rabi frequency of 8 MHz

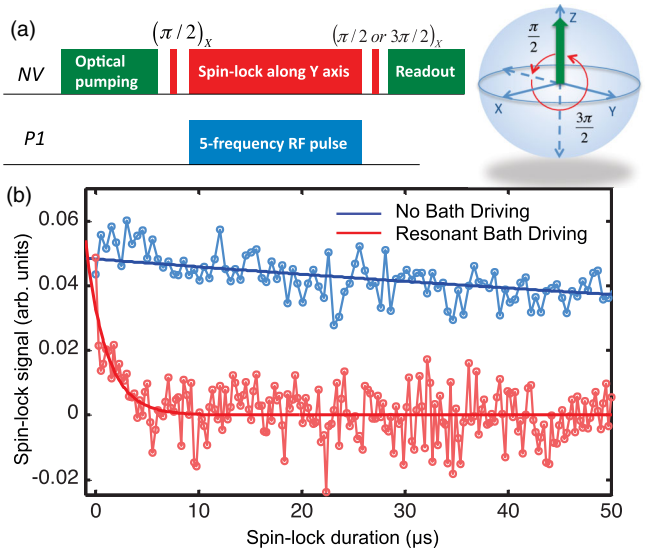

FIG. 3 (color online). Measured dressed-state NV-$P1$ resonant coupling. (a) NV optical and microwave spin-lock sequence, and timing of five-frequency rf pulse to drive $P1$ spin bath. After initializing NVs to the the $|m_s = 0\rangle$ state (Z axis) with a 2 μs optical pumping pulse, $\pi/2$ and $3\pi/2$ microwave pulses are applied along the X axis to rotate the spin to or from the equator of the Bloch sphere, and a microwave spin-locking pulse of variable duration is applied along the Y axis. To bring the $P1$ bath into dressed-state resonance with the NV spins, a five-frequency rf pulse is applied during the spin-lock duration. (b) Measured decay of NV spin-lock signal as a function of spin-lock duration. When the $P1$ bath is not driven we record the blue trace. Driving the $P1$ bath simultaneously at all five ESR resonances such that the collective $P1$-bath Rabi frequency equals the NV Rabi frequency (8 MHz) gives the red trace, indicating strong NV spin depolarization caused by NV-$P1$ resonant coupling. Solid lines represent fits to decaying exponentials (see the Supplemental Material [25]).

(matched to the $P1$ Rabi frequency). Measuring the NV spin-lock signal as a function of the duration of the spin-lock pulse with no rf signal applied, we found the rotating-frame spin-lattice relaxation time $T_{1,\rho} = 290(50)$ μs. The blue trace of Fig. 3(b) shows the first 50 μs of this measured NV spin-lock signal. When the $P1$ spin bath was driven such that the collective Rabi frequency was also 8 MHz, we observed an $\sim 100\times$ faster decay of the NV spin-lock signal with rotating-frame spin-lattice relaxation time under resonant-coupling conditions $T_{1,\rho}^{\mathrm{RC}} = 2.0(4)$ μs, as shown by the red trace of Fig. 3(b). This dramatic effect demonstrates that in the rotating frame the NV spins are much more strongly coupled to the $P1$ spin bath under the condition of matched $P1$ and NV Rabi frequencies. At dressed-state resonance, polarization may be transferred back and forth between the NV and the bath several times before the NV is completely depolarized. Thus while the time scale for each energy conserving flip-flop is $\sim T_2^*$, the depolarization time scale can be much longer. Experimentally, we observe depolarization on a time scale $T_{1,\rho}^{\mathrm{RC}}$ which is approximately equal to T_2 in the lab (nonrotating) frame.

To verify that the rapid decay of the NV spin-lock signal was caused by resonant coupling to the $P1$ spins, we set the NV Rabi frequency to 8 MHz and the spin-lock duration to 50 μs, drove the $P1$ spin bath at a Rabi frequency of 8 MHz (at a single rf frequency instead of all five), and slowly swept the rf frequency past the five $P1$-bath ESR resonances. Each time the rf frequency equaled that of a $P1$-bath resonance, we observed a drop in the NV spin-lock signal [see Fig. 4(a)] consistent with enhanced NV-spin coupling and polarization transfer to the $P1$ spin bath. Through this measurement we could also infer

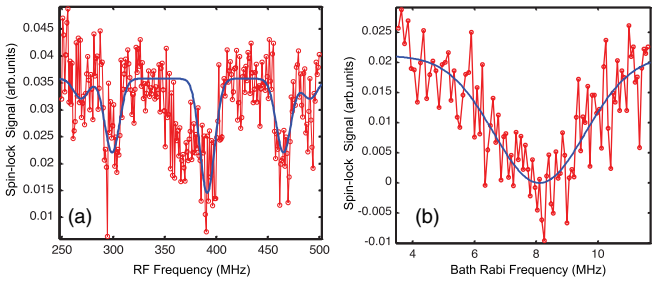

FIG. 4 (color online). Measured spectrum of NV-spin resonant coupling to $P1$ bath spins. Here $B_0 = 132$ gauss and the NV Rabi frequency $= 8$ MHz. (a) A single-frequency rf signal, with power corresponding to $P1$ Rabi frequency of 8 MHz, is swept across the $P1$-bath resonances. When the rf frequency equals that of a $P1$-spin-bath resonance, the NV spin-lock signal is reduced. Solid line is a fit to a set of five Gaussians (see the Supplemental Material [25]). (b) NV-$P1$ dressed-state resonance spectrum is measured by monitoring the NV spin-lock signal, applying rf power at the central $P1$-bath resonance dip, and sweeping the power of the rf signal. Solid line represents a Gaussian fit (see the Supplemental Material [25]). The resonance is centered at 8.1(1) MHz and has a FWHM of 3.5(4) MHz.

resonant coupling to the unknown electronic spin impurity. We next characterized the NV-$P1$ dressed-state resonance spectrum by setting the NV Rabi frequency to 8 MHz and the spin-lock duration to 50 μs, setting the rf signal frequency to that of the central ESR dip of the $P1$ spin bath, and scanning the rf power to tune the $P1$-bath Rabi frequency through the dressed-state resonance condition. When the rf power was such that the $P1$ and NV Rabi frequencies were equal (8 MHz), we observed a reduction in the NV spin-lock signal as shown in Fig. 4(b). This NV-$P1$ dressed-state resonance is broadened by dipolar coupling between $P1$ spins with a width approximately equal to $1/\pi T_2^*$.

When the resonant coupling condition of matched Rabi frequencies is satisfied, polarization is transferred from NV spins to the neighboring $P1$ spins and then out to the large bath of $P1$ spins. To apply this scheme to achieve high spin polarization of multiple dark $P1$ spins nearby to bright NV spins as a resource for quantum information, sensing, and metrology, repeated NV-initialization and NV-$P1$-polarization transfer cycles will be required. Also, the achievable $P1$-bath spin polarization will be limited by the $P1$ spin-lattice relaxation time, which is ~ 1 ms in room-temperature diamond [17]. Since NV-$P1$ polarization transfer takes place within ~ 2 μs as shown above, it should be possible to perform several hundred polarization cycles before the $P1$ spins relax. An important factor that limits the achievable $P1$-bath spin polarization in the present experiment is spin-diffusion between closely spaced $P1$ spins. This limitation may be overcome, for example, by restricting the size of the spin bath by confining it within submicron structures [26], or by realizing a higher ratio of optically bright NV centers (polarization sources) to dark $P1$ spins to be polarized. Such approaches will be the subject of future work.

In conclusion, we demonstrated that matching drive Rabi frequencies enables resonant coupling between optically bright NV electronic spins and nearby dark $P1$ electronic spins in room-temperature diamond, even when the strength of the NV-$P1$ interaction is not known or is inhomogeneous. With optimized samples, such dressed-state resonant coupling will enable mesoscopic ensembles of dark spins to be polarized with optical control and at arbitrary magnetic fields, opening up several exciting possibilities. Chains of polarized dark spins could be used to enable coherent state transfer between distant NVs [13,14,27]. Environmentally enhanced magnetometry, where the dark spins are used for field sensing, could increase the sensitivity of NV-based magnetometers [15,28]. The resonant-coupling mechanism described here could also be extended to detect and polarize spins external to the diamond and thus enable single-molecule magnetic-resonance spectroscopy [16,29] and diamond-based quantum simulations [30].

This work was supported by NIST, NSF and DARPA (QuEST and QuASAR programs). We gratefully acknowledge the provision of diamond samples by Apollo, and helpful technical discussions with Stephen DeVience, Michael Grinolds, Patrick Maletinsky, Ashok Ajoy, Alexandre Cooper, Mikhail Lukin, Amir Yacoby, and Fedor Jelezko.

*rwalsworth@cfa.harvard.edu

[1] T. D. Ladd, F. Jelezko, R. Laflamme, Y. Nakamura, C. Monroe, and J. L. O'Brien, Nature (London) **464**, 45 (2010).
[2] J. M. Taylor, P. Cappellaro, L. Childress, L. Jiang, D. Budker, P. R. Hemmer, A. Yacoby, R. Walsworth, and M. D. Lukin, Nat. Phys. **4**, 810 (2008).
[3] C. L. Degen, Appl. Phys. Lett. **92**, 243111 (2008).
[4] J. R. Maze *et al.*, Nature (London) **455**, 644 (2008).
[5] G. Balasubramanian *et al.*, Nature (London) **455**, 648 (2008).
[6] J. H. N. Loubser and J. A. van Wyk, Rep. Prog. Phys. **41**, 1201 (1978).
[7] G. de Lange, Z. H. Wang, D. Riste, V. V. Dobrovitski, and R. Hanson, Science **330**, 60 (2010).
[8] C. A. Ryan, J. S. Hodges, and D. G. Cory, Phys. Rev. Lett. **105**, 200402 (2010).
[9] B. Naydenov, F. Dolde, L. T. Hall, C. Shin, H. Fedder, L. C. L. Hollenberg, F. Jelezko, and J. Wrachtrup, Phys. Rev. B **83**, 081201 (2011).
[10] N. Bar-Gill, L. M. Pham, C. Belthangady, D. Le Sage, P. Cappellaro, J. R. Maze, M. D. Lukin, A. Yacoby, and R. Walsworth, Nat. Commun. **3**, 858 (2012).
[11] G. de Lange, T. van der Sar, M. Blok, Z.-H. Wang, V. Dobrovitski, and R. Hanson, Sci. Rep. **2**, 382 (2012).
[12] L. M. Pham, N. Bar-Gill, C. Belthangady, D. Le Sage, P. Cappellaro, M. D. Lukin, A. Yacoby, and R. L. Walsworth, Phys. Rev. B **86**, 045214 (2012).
[13] S. Bose, Phys. Rev. Lett. **91**, 207901 (2003).
[14] N. Y. Yao, L. Jiang, A. V. Gorshkov, Z. X. Gong, A. Zhai, L. M. Duan, and M. D. Lukin, Phys. Rev. Lett. **106**, 040505 (2011).
[15] G. Goldstein, P. Cappellaro, J. R. Maze, J. S. Hodges, L. Jiang, A. S. Sorenson, and M. D. Lukin, Phys. Rev. Lett. **106**, 140502 (2011).
[16] J.-M. Cai, F. Jelezko, M. B. Plenio, and A. Retzker, New J. Phys. **15**, 013020 (2013).
[17] S. Takahashi, R. Hanson, J. van Tol, M. S. Sherwin, and D. D. Awschalom, Phys. Rev. Lett. **101**, 047601 (2008).
[18] T. Gaebel *et al.*, Nat. Phys. **2**, 408 (2006).
[19] R. Hanson, F. M. Mendoza, R. J. Epstein, and D. D. Awschalom, Phys. Rev. Lett. **97**, 087601 (2006).
[20] S. R. Hartmann and E. L. Hahn, Phys. Rev. **128**, 2042 (1962).
[21] M. Poggio, H. J. Mamin, C. L. Degen, M. H. Sherwood, and D. Rugar, Phys. Rev. Lett. **102**, 087604 (2009).
[22] E. C. Reynhardt and G. L. High, J. Chem. Phys. **109**, 4100 (1998).
[23] W. V. Smith, P. P. Sorokin, I. L. Gelles, and G. Lasher, Phys. Rev. **115**, 1546 (1959).
[24] C. P. Slichter, *Principles of Magnetic Resonance* (Springer-Verlag, Berlin, 1990).
[25] See Supplemental Material http://link.aps.org/supplemental/10.1103/PhysRevLett.110.157601 for additional experimental details and the procedure used for data analysis.
[26] T. M. Babinec, B. J. M. Hausmann, M. Khan, Y. Zhang, J. R. Maze, P. R. Hemmer, and M. Lončar, Nat. Nanotechnol. **5**, 195 (2010).
[27] P. Cappellaro, L. Viola, and C. Ramanathan, Phys. Rev. A **83**, 032304 (2011).
[28] P. Cappellaro, G. Goldstein, J. S. Hodges, L. Jiang, J. R. Maze, A. S. Sørensen, and M. D. Lukin, Phys. Rev. A **85**, 032336 (2012).
[29] D. Rugar, R. Budakian, H. J. Mamin, and B. W. Chui, Nature (London) **430**, 329 (2004).
[30] J.-M. Cai, A. Retzker, F. Jelezko, and M. B. Plenio, Nat. Phys. **9**, 168 (2013).
[31] A. Laraoui, J. S. Hodges, and C. A. Meriles, Nano Lett. **12**, 3477 (2012).